JOURNAL OF AGRICULTURAL AND FOOD CHEMISTRY

Micrometer-Sized Fibrillar Protein Aggregates from Soy Glycinin and Soy Protein Isolate

C. AKKERMANS,[†,‡] A. J. VAN DER GOOT,[*,†] P. VENEMA,[‡] H. GRUPPEN,[§] J. M. VEREIJKEN,[⊥] E. VAN DER LINDEN,[‡] AND R. M. BOOM[†]

Food and Bioprocess Engineering Group, Food Physics Group, Laboratory of Food Chemistry, Wageningen UR, PO Box 8129, 6700 EV Wageningen, The Netherlands, and Agrotechnology and Food Sciences Group, Wageningen UR, PO Box 17, 6700 AA Wageningen, The Netherlands

Long, fibrillar semiflexible aggregates were formed from soy glycinin and soy protein isolate (SPI) when heated at 85 °C and pH 2. Transmission electron microscopy analysis showed that the contour length of the fibrils was ~1 μm, the persistence length 2.3 μm, and the thickness a few nanometers. Fibrils formed from SPI were more branched than the fibrils of soy glycinin. Binding of the fluorescent dye Thioflavin T to the fibrils showed that β-sheets were present in the fibrils. The presence of the fibrils resulted in an increase in viscosity and shear thinning behavior. Flow-induced birefringence measurements showed that the behavior of the fibrils under flow can be described by scaling relations derived for rodlike macromolecules. The fibril formation could be influenced by the protein concentration and heating time. Most properties of soy glycinin fibrils are comparable to β-lactoglobulin fibrils.

KEYWORDS: Soy glycinin; soy protein isolate; aggregation; fibrils; birefringence; TEM; Thioflavin T; viscosity

INTRODUCTION

Many proteins of animal origin give rise to aggregation into long, semiflexible aggregates. These types of aggregates are interesting as ingredients in food products because they are able to modify various physical properties, such as viscosity, flow behavior, and gelation on a weight efficient basis. Examples of proteins that can form these fibrils are β-lactoglobulin (*1*–*5*), ovalbumin (*6*), BSA, (*7*) and lysozyme (*8*). Since plants are a more sustainable protein source than animals, it becomes interesting to study the capability of plant proteins to form these fibrils.

The most abundant food protein studied with respect to fibril formation is β-lactoglobulin, which aggregates into long, semiflexible fibrils upon heating above the denaturation temperature, at low pH and low ionic strength (*1*–*5*). The length of the fibrils obtained ranges from 1 to 10 μm, and the thickness is on the order of a few nanometers (*2*). Factors that influence the fibril formation are protein concentration, heating time, and shearing or stirring during heating (*9*–*11*). Fibrils with a similar morphology could also be formed from whey protein isolate (WPI) (*12*), which is a more relevant starting material from an industrial point of view.

Soybeans contain two major storage proteins: glycinin and β-conglycinin. Glycinin consists of five different subunits (MW ~20 000–36 000 Da) (*13, 14*) and is completely denatured when heated at 85 °C at pH 3.8 and low ionic strength (*15*). β-Conglycinin has three subunits (MW ~45–72 kDa) (*16*). Although long (>1 μm) fibrillar soy protein aggregates have not yet been observed, there have been some studies on the heat-induced gelation of soy protein above and below the isoelectric point. Puppo et al. (*17*) showed that transparent soy protein isolate gels were formed at pH 2.75 and pH 8 (which hints in the direction of strandlike aggregates). Hermansson (*18*) observed gels containing shorts strands (~100 nm) after heating at pH 7, for both glycinin gels and β-conglycinin-rich gels.

In this paper, we show that micrometer-sized fibrillar aggregates can be formed from soy glycinin and soy protein isolate. Since most information is available on β-lactoglobulin/WPI fibrils, we compare the properties of soy protein fibrils with the properties of β-lactoglobulin fibrils. The results described in this paper include a physical characterization of soy glycinin fibrils with the use of transmission electron microscopy (TEM), flow-induced birefringence, viscosity measurements, and Thioflavin T (ThT) fluorescence. The effect of different parameters (heating time, concentration, and applying shear flow) on the fibril concentration of soy glycinin is explored. Furthermore, the effect of using SPI instead of soy glycinin to obtain these fibrils is studied.

MATERIALS AND METHODS

Soy Protein Isolation: Glycinin and Soy Protein Isolate. This protein isolation method was adapted from Kuipers et al. (*19, 20*). Soybean meal was prepared by milling soybeans (Hyland soybeans,

* To whom correspondence should be addressed (telephone +31 317 484372; fax +31 317 482237; e-mail atzejan.vandergoot@wur.nl).
[†] Food and Bioprocess Engineering Group.
[‡] Food Physics Group.
[§] Laboratory of Food Chemistry.
[⊥] Agrotechnology and Food Sciences Group.

10.1021/jf0718897 CCC: $37.00
Published on Web 10/30/2007

Table 1. Overview of Heating Conditions Used during This Study (All Samples Were Heated at 85 °C and pH 2)

protein	conc (g L^{-1})	time (h)	shear flow[a]	
glycinin	10	2	+	−
	10	20	+ (3)[b]	− (2)
	20	2	+	−
	20	20	+ (6)	−
	40	2	+	−
	40	20	+ (5)	−
SPI	40	20	+	

[a] Shear flow was applied during heating at a shear rate of 323 s^{-1} (+) or samples were heated without the use of shear flow (−). [b] The amount of replicate experiments is indicated between parentheses.

Fa. L.I. Frank, Twello, The Netherlands) in a Fritsch Pulverisette 14702. First, a 4 mm sieve was used and then a 0.5 mm sieve (Fritsch Gmb, Albisheim, Germany). Milling was performed in the presence of liquid N_2 to prevent excessive heating. The soybean meal was defatted five times with hexane at room temperature (w/v ratio SBM/hexane 1:5) followed by drying in air. Hexane was removed from the suspension by filtration.

To isolate the soy protein, a protein extract was prepared by suspending the soybean meal (145 g of meal in 1.5 L of buffer) in a 30 mM Tris-HCl buffer (pH 8), containing 10 mM 2-mercaptoethanol. The suspension was stirred at room temperature for 1.5 h, followed by centrifugation (30 min, 20 °C, 19 000*g*, Beckman) and filtration (Whatman, Schleicher & Schuell, type 595½) to remove the insoluble parts.

To obtain soy glycinin, the supernatant was set to pH 6.4 to induce precipitation of glycinin. After stirring for 1 h, the suspension was centrifuged (30 min, 20 °C, 19 000*g*, Beckman). The precipitate was resuspended and adjusted to pH 8. After stirring overnight, the protein solution was centrifuged (30 min, 20 °C, 19 000*g*, Beckman), and the supernatant was dialyzed (MWCO 12 000–14 000; Visking, Medicell International Ltd.) against demineralized water to remove electrolytes. The pH of the dialyzed solution was set to 8 and the solution was freeze-dried.

To obtain soy protein isolate (SPI), the supernatant of the pH 8 protein extract described above was set to pH 4.8 to induce precipitation of soy proteins. After stirring for 1 h, the suspension was centrifuged (30 min, 20 °C, 19 000*g*, Beckman). The precipitate was washed twice with Millipore water, and after each washing step, the suspension was centrifuged. The precipitate was resuspended and set to pH 8. After stirring overnight and resetting the pH to 8, the solution was freeze-dried.

The protein content of the isolates was measured using Dumas analysis, using a nitrogen factor of 5.56 for soy glycinin and 5.71 for SPI. The protein content varied between 82 and 88%. The protein composition of soy glycinin and SPI was determined using high-pressure size exclusion chromatography according to the method described by Kuipers et al. (*20*). Different batches of isolated glycinin were used during this study, and the glycinin content of the batches was between 90 and 94%; the remaining part consisted primarily of β-conglycinin. SPI consisted of 80% glycinin and ~20% β-conglycinin.

Protein Stock Solutions. Protein stock solutions of glycinin and SPI were made by dissolving the protein in Millipore water. The pH of the solutions was set to 2 by adding a concentrated HCl solution, followed by centrifugation (30 min, 4 °C, 15 000*g*, Beckman) and filtration (Minisart, Sartorius, 0.45 μm for soy glycinin, and 1.2 μm for SPI) to remove undissolved protein. The protein concentration of the solutions was measured using Dumas analysis, using a nitrogen factor of 5.56 for soy glycinin and 5.71 for SPI.

Sample Preparations. All samples were heated at 85 °C at pH 2 in a titanium shearing device with Couette geometry. Details of this shearing device have been described in a previous paper (*9*). The following conditions were used to prepare the samples: heating time of 2 or 20 h, protein concentration of 10, 20, or 40 g L^{-1}, and quiescent conditions or shear flow (shear rate of 323 s^{-1}). One sample was prepared from SPI; the rest were prepared from soy glycinin. **Table 1** gives an overview of all experiments, and some were performed multiple times to study the experimental variation.

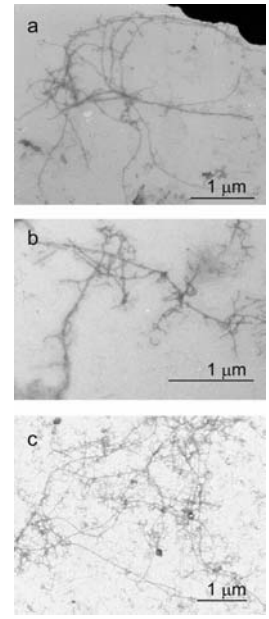

Figure 1. TEM pictures of soy protein fibrils (heating conditions: 20 h, 85 °C, with shear flow, pH 2): (**a**) fibrils prepared from soy glycinin (20 g protein L^{-1}), (**b**) fibrils prepared from soy glycinin (40 g protein L^{-1}), (**c**) fibrils prepared from SPI (40 g protein L^{-1}).

Flow-Induced Birefringence. Flow-induced birefringence was measured on a strain-controlled ARES rheometer (Rheometric Scientific) with Couette geometry (rotating cup with a diameter of 33.8 mm and a static bob with a diameter of 30.0 mm). A laser beam of wavelength 670 nm passed vertically through the gap between the cup and the bob. The birefringence was measured with a modified optical analysis module (*21*).

The flow-induced birefringence of all samples was measured at a shear rate of 73 s^{-1} for 30 s to characterize the fibril length concentration. For one sample (heating conditions: 20 g protein L^{-1}, 20 h, with shear flow), steady shear rate sweeps from 0.01 to 100 s^{-1} were performed on three dilutions of this sample (undiluted, 1.2× diluted, and 1.6× diluted). Each shear rate was applied for 30 s, which was sufficient to obtain a steady birefringence signal.

Fibril Concentration from Flow-Induced Birefringence. In order to measure the fibril concentration (amount of proteins aggregated into fibrils), the birefringence signal, Δn, was measured at a shear rate of 73 s^{-1} (see previous section for a description of the birefringence measurement). Assuming full alignment of the fibrils, the birefringence signal could be converted into the fibril concentration using eq 1 (*22*):

$$\Delta n = M \int c_L \, dL \tag{1}$$

The constant M (m^2), which depends on the anisotropy in polarizability per unit fibril length, is necessary to convert the birefringence, Δn, into the total fibril length concentration, $c_{L,tot}$ (m^{-2}) ($c_{L,tot} = \int c_L \, dL$). Equation 2 describes the relation between the total fibril length concentration and the fibril concentration, c_{fib} (in g m^{-3}).

$$c_{L,tot} = c_{fib} N_a / (l_{fib} M_w) \tag{2}$$

In eq 2, N_a is Avogadro's number and M_w is the molecular mass for which we used 24 700 Da (assuming equal proportions of the five major subunits were present in the fibrils). For the fibril line density (l_{fib}), the same value that was determined for β-lactoglobulin fibrils was used (0.28×10^9 m^{-1}) (*23*) because the thickness of the glycinin fibrils seems comparable to β-lactoglobulin fibrils (see **Figure 1a**).

To be able to use the birefringence signal to calculate the fibril concentration, the value of M is needed for soy glycinin fibrils.

Therefore, fibrils and proteins were separated, and the amount of protein that was not present in the fibrils was measured. Since this analysis is time-consuming, it was only done for four samples (heating conditions: protein concentration of 20 g L^{-1}, 20 h, with shear flow). The samples were diluted to a protein concentration of 1 g L^{-1}, and 2 mL of these diluted samples was filtered using centrifugal filter units (MWCO 100 000; Centricon YM-100, Millipore) (1000*g* for 30 min at 20 °C). The retentate was washed twice with pH 2 solution after each centrifugation run to remove nonaggregated protein left in the retentate. The amount of nonaggregated protein was determined from the amount of protein present in the filtrates using Dumas analysis. In the third filtrate, no protein was detected anymore. The difference between the total amount of protein and nonaggregated protein was used as the amount of protein aggregated into fibrils. The amount of protein aggregated into fibrils of these four samples was between 2.5 and 4.3 g L^{-1}, and the constant M was calculated to be 2.8×10^{-20} m^2 (using the average fibril concentration and average birefringence of these samples). For whey protein isolate fibrils, a comparable value for M was determined (3.3×10^{-20} m^2) using the same method to separate fibrils and proteins (*24*).

Transmission Electron Microscopy. TEM grids were prepared by negative staining immediately after the preparation of the samples. The samples were diluted, and a droplet of the diluted sample was put onto a carbon support film on a copper grid. After 15 s, the droplet was removed with a filter paper. Then, a droplet of 2% uranyl acetate was put onto the grid and removed after 15 s. The micrographs were made using a Philips CM 12 electron microscope operating at 80 kV.

Determination of Persistence Length. The persistence length of seven fibrils was determined from the TEM pictures. The contour of the fibrils in the TEM picture was digitized using a polynomial function (8th or 10th order). The average correlation, $\langle u(s)\, u(s')\rangle$, was determined for different segment lengths ($s - s'$) along the fibrils. The persistence length, L_p, was determined by fitting eq 3 to the segment lengths. This equation describes the correlation of wormlike chains in two dimensions (*25*):

$$\langle u(s)\, u(s')\rangle = \exp\left(-\frac{s-s'}{2L_p}\right) \quad (3)$$

Viscosity. Flow curves were measured on a stress-controlled rheometer (Anton Paar, Physica, MCR 301) with a Couette geometry. Steady shear viscosities were measured for shear rates from 0.01 to 100 s^{-1}. Each shear rate was applied for 120 s up to a shear rate of 1 s^{-1}; above this shear rate, each rate was applied for 30 s. Only data points were used for which a steady state viscosity was obtained after 30 or 120 s.

Thioflavin T Fluorescence. A Thioflavin T solution (18 mg L^{-1}) was prepared by dissolving Thioflavin T (Merck-Schuchardt) in a phosphate buffer (10 mM phosphate, 150 mM NaCl at pH 7.0), and the solution was filtered (Minisart, Sartorius, 0.2 μm) to remove undissolved ThT. Samples of 24 μL were added to 4 mL of the ThT solution. The fluorescence of the samples was measured using a luminescence spectrophotometer (LS50B, Perkin-Elmer). ThT was excited at a wavelength of 460 nm, and the emission of the sample (I_{ThT}) was measured at 486 nm.

RESULTS

Characterization of Soy Glycinin Fibrils. In this section, we show that micrometer-sized, semiflexible fibrils can be formed from soy glycinin. Fibrils were formed after heating a soy glycinin solution for 20 h with shear flow, at 85 °C and pH 2. In **Figure 1**, TEM pictures are shown of the fibrils after heating soy glycinin solutions of 20 g protein L^{-1} (**Figure 1a**) and 40 g protein L^{-1} (**Figure 1b**). Long fibrils were formed with a diameter of a few nanometers, which were slightly branched and curved. No clear differences were observed in fibril morphology when the fibrils were prepared at different protein concentrations. When Thioflavin T was added to the fibril solution, an increase in fluorescent emission (measured at a wavelength of 486 nm) was observed. **Table 2** shows the measured intensity for the soy glycinin fibrils. This increase in emission shows that β-sheets were present in the fibrils to which Thioflavin T was bound.

Table 2. Birefringence Signals (Measured at a Shear Rate of 73 s^{-1}) and ThT Fluorescence Emission (Measured at 486 nm) of Soy Glycinin and SPI Solutions (Heating Conditions: 40 g Protein L^{-1}, 20 h, 85 °C, with Shear Flow, pH 2)

protein	Δn	I_{ThT}
soy glycinin	$(29 \pm 0.2) \times 10^{-6}$	508 ± 19
SPI	$(13 \pm 0.1) \times 10^{-6}$	972 ± 19[a]

[a] This value was extrapolated from a 2× diluted sample ($I_{ThT} = 486$) because the undiluted sample was outside the linear range of the spectrophotometric analysis.

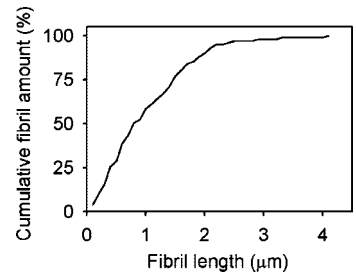

Figure 2. Cumulative fibril length distribution of soy glycinin fibrils obtained by measuring fibril length ($N = 101$) from TEM pictures (heating conditions of sample: 20 g protein L^{-1}, 20 h, 85 °C, with shear flow, pH 2).

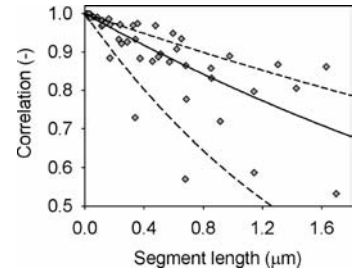

Figure 3. Correlation $\langle u(s)\, u(s')\rangle$ versus segment length ($s - s'$) for all fibrils for which the persistence length was determined ($N = 7$). The lines represents the correlation according to eq 3 for which the average persistence length (2.3 μm) was used (solid line) and average length plus or minus the standard deviation (1.4 μm) (dotted lines).

Figure 2 shows the fibril length distribution that was obtained from the TEM pictures by measuring the contour lengths of the soy glycinin fibrils ($n = 101$). The average fibril length was 1.1 μm, while the measured fibril lengths ranged from 0.1 to 4 μm, which shows that the fibril length was polydisperse. The persistence length of the fibrils was measured by determining the average correlation, $\langle u(s)\, u(s')\rangle$, of different segment lengths ($s - s'$) along the fibrils ($N = 7$). **Figure 3** shows the correlations for different segment lengths of all fibrils. A persistence length was determined for each fibril. The average persistence length was 2.3 ± 1.4 μm, and the correlation for this average fibril length using eq 3 is depicted in **Figure 3**. The measured correlations of the different fibrils are scattered around this average correlation. This analysis shows that the persistence length of the fibrils is comparable to the contour length, which is generally observed in the case of semiflexible fibrils.

The behavior of the fibrils in solution was measured using flow-induced birefringence and viscosity measurements. In the case of the birefringence measurements, concentration scaling for rods in the dilute and semidilute regime was applied (Doi–Edwards theory). In the dilute regime, rods diffuse unhindered of each other, resulting in a rotational diffusion coefficient, D_r, for rods that is independent of the concentration,

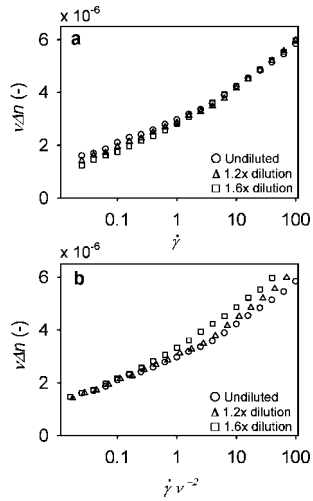

Figure 4. Dilute (**a**) and semidilute scaling (**b**) of three dilutions of one soy glycinin fibril solution (heating conditions: 20 g protein L^{-1}, 20 h, 85 °C, with shear flow, pH 2). Birefringence signals were multiplied by the dilution factor, v, and for semidilute scaling, the shear rate was divided by v^2.

c. In the semidilute regime, rods start to overlap with each other, resulting in a rotational diffusion coefficient that is dependent on the concentration ($D_r \sim c^{-2}$) (*26*). Flow-induced birefringence can be used to test this concentration scaling because the degree of alignment of the rods depends on the rotational diffusion and the applied shear rate. Flow-induced birefringence of a soy glycinin fibril solution was measured at different shear rates and three different dilutions of this sample (undiluted, 1.2× dilution, and 1.6× dilution). In the case of the dilute concentration regime, plotting the birefringence multiplied by the dilution factor, v, should put the curves of the three diluted samples onto one master curve because in this concentration regime, the rotational diffusion is independent of the concentration (*22*). In the case of the semidilute concentration regime, plotting the data according to eq 4 should put the curves onto one master curve because in this concentration regime, the rotational diffusion depends on the protein concentration (*22*).

$$v\Delta n = \dot{\gamma} v^{-2} \quad (4)$$

Figure 4a shows the birefringence signals of the three diluted fibril solutions as a function of shear rate. The birefringence increased as a function of shear rate, which shows that an increasing shear rate resulted in more alignment of the fibrils. For high shear rates, the curves of the three diluted fibril solutions overlapped, which means that for high shear rates the fibrils scale like rods in the dilute concentration regime. **Figure 4b** shows the same data, but scaled according to rods in the semidilute concentration regime. At low shear rates, the curves of the three diluted fibril solutions overlapped, and this means that the fibrils scale like rods in the semidilute concentration regime at low shear rates. This analysis shows that the soy glycinin fibrils scale like rods in the dilute (high shear rates) and semidilute (low shear rates) concentration regime. This behavior was also observed for β-lactoglobulin fibrils by Rogers et al. (*22*), and they explained that the multiple scaling could be caused by the polydisperse fibril length. At low shear rates, only long fibrils (which are in the semidilute regime) were aligned, while upon further increasing the shear rate, smaller fibrils (which are in the dilute regime) became aligned.

Figure 5 shows viscosity measurements of the samples of **Figure 4**, together with the viscosity of an unheated soy glycinin solution at pH 2. The presence of the fibrils resulted in a clear

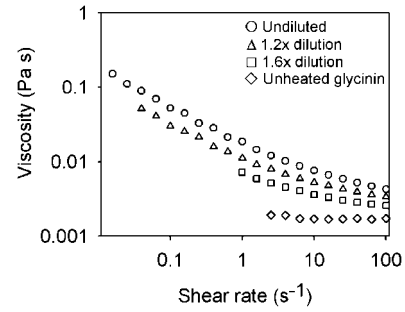

Figure 5. Viscosity plotted versus shear rate for the three dilutions of one sample (heating conditions: see **Figure 4**) and an unheated glycinin solution (20 g L^{-1}, pH 2).

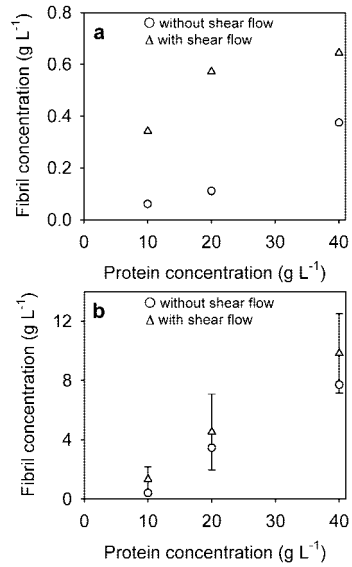

Figure 6. Fibril concentration versus protein concentration for samples of soy glycinin heated for (**a**) 2 h and (**b**) 20 h, prepared with and without shear flow. Please note the difference in scaling of (**a**) and (**b**).

increase in viscosity compared to the unheated sample. All dilutions showed shear thinning behavior, and the viscosity decreased when less fibrils were present. At high shear rates, the viscosity started to approach the viscosity of the solvent (0.001 Pa s).

Factors Influencing the Formation of Soy Glycinin Fibrils. Three different parameters (protein concentration, heating time, and shear flow) were varied to study the influence of heating conditions on the formation of soy glycinin fibrils. The fibril concentration in the samples was determined from flow-induced birefringence measurements at a shear rate of 73 s^{-1}. **Figure 6a**,**b** shows the fibril concentrations as a function of the protein concentration of the samples heated for 2 h (**a**) and 20 h (**b**). Some of the samples were prepared using shear flow, while the others were prepared without shear flow. Heating for 20 h was performed multiple times, and the standard deviations of these measurements are indicated by the error bars. The variation in the results is rather large, but despite this variation, some trends can be observed. A higher protein concentration or a longer heating time resulted in a higher fibril concentration. The use of shear flow did not have a significant effect when a heating time of 20 h was used. When a heating time of 2 h was used, shear flow seems to enhance the fibril formation.

Fibrils of Soy Protein Isolate (SPI). Figure 1c shows a TEM picture of fibrils obtained by heating an SPI solution (containing 80% soy glycinin and 20% β-conglycinin) of 40 g protein L^{-1} for 20 h, with shear flow, at 85 °C and pH 2. The length of the

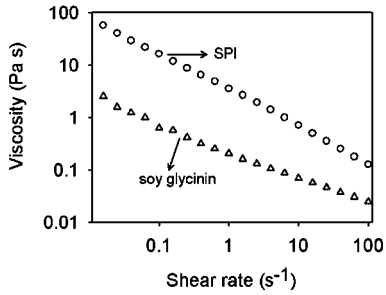

Figure 7. Flow curves of soy glycinin and SPI fibril solutions (heating conditions: 40 g protein L^{-1}, 20 h, 85 °C, with shear flow, pH 2).

SPI fibrils was in the order of 1 μm, which is similar to the soy glycinin fibrils. SPI fibrils were more branched than the soy glycinin fibrils (see **Figure 1a**,**b**).

Differences in fibril concentration between soy glycinin and SPI were measured using flow-induced birefringence and Thioflavin T fluorescence. **Table 2** shows the values for samples containing SPI and soy glycinin fibrils (both heated for 20 h at 85 °C, with shear flow, and a protein concentration of 40 g L^{-1}). As previously observed for soy glycinin fibrils, the presence of SPI fibrils also resulted in an increase in Thioflavin T fluorescent emission (measured at 486 nm). This confirms that β-sheets were present in the SPI fibrils to which Thioflavin T was bound. The ThT fluorescence intensity of the sample containing SPI fibrils was higher than the intensity of the sample containing soy glycinin fibrils, while the birefringence of the sample containing SPI fibrils was lower than the birefringence of the sample containing soy glycinin fibrils. Since both the birefringence and the ThT fluorescence intensity are a measure of the fibril concentration, it seems that the responses of the two methods are different for SPI than for soy glycinin. On the basis of the TEM pictures, we conclude that the SPI fibrils are less prone to alignment than the soy glycinin fibrils due to their branches, which resulted in a lower birefringence signal for SPI fibrils. The higher ThT fluorescence intensity for SPI fibrils indicates that for these two specific samples more protein was incorporated into the SPI fibrils than into the soy glycinin fibrils.

Figure 7 shows the flow curves of soy glycinin and SPI fibrils. Both samples were shear thinning, and the viscosity of the SPI fibril solution was higher than the viscosity of the soy glycinin solution. This higher viscosity for SPI fibrils was probably caused by the higher amount of protein present in the fibrils.

DISCUSSION

In this discussion, we will compare soy protein fibrils with fibrils of β-lactoglobulin and WPI fibrils because much information is available about these fibrils, and WPI is an industrially relevant mixture of proteins.

Compared to β-lactoglobulin and WPI, the morphology of soy glycinin and SPI fibrils is partly similar because β-lactoglobulin and WPI can also form micrometer-sized, semiflexible fibrils with a diameter of a few nanometers (*1*, *2*, *4*, *5*, *9*, *12*). Furthermore, Thioflavin T can also bind to the β-sheets present in β-lactoglobulin and WPI fibrils (*24*, *27*). The persistence length of soy glycinin is similar to the persistence length of β-lactoglobulin fibrils (*28*). Birefringence measurements showed that the behavior of soy glycinin fibrils under flow can be described by scaling relations derived for rodlike macromolecules, and viscosity measurements showed that the presence of soy glycinin fibrils resulted in an increase in viscosity and shear thinning behavior. Previous research showed similar behavior under flow for β-lactoglobulin and WPI fibrils (*9*, *11*, *22*).

The fibril concentration of soy glycinin could be influenced by the protein concentration, heating time, and use of shear flow during heating. Previous studies on WPI fibrils showed that the WPI fibril concentration could also be influenced by the same factors (*9*, *11*).

So far, we have addressed the similarities between fibrils formed from SPI and soy glycinin and fibrils formed from WPI and β-lactoglobulin. However, there are also some differences. A large experimental variation in fibril concentration was observed for soy glycinin fibrils (**Figure 6**), and partly, this has also been observed for fibrils formed from WPI (*9*). However, the variation seems larger for soy glycinin fibrils, which could be caused by the heterogeneous nature of soy glycinin (*13*, *14*).

Fibrils of soy glycinin and SPI fibrils are more branched than fibrils of β-lactoglobulin and WPI fibrils when they are prepared at similar conditions (heating at pH 2 at a protein concentration of 50 g/L or lower) (*4*, *9*). Furthermore, SPI fibrils were more branched than soy glycinin fibrils. The difference between soy glycinin and SPI is a higher concentration of β-conglycinin, which means that this protein influences the morphology of SPI fibrils. Further research should clarify the role of β-conglycinin on the morphology of soy protein fibrils. In the case of WPI, no differences have been observed in morphology compared to β-lactoglobulin, and β-lactoglobulin seems to be the only whey protein that is incorporated into WPI fibrils (*12*).

To summarize, many properties of soy protein fibrils are similar to β-lactoglobulin and WPI fibrils, which makes them possible candidates as sustainable structural ingredients in food products. In particular, the high viscosity and shear thinning behavior of soy protein fibrils show that they have a promising ability to modify physical properties.

ACKNOWLEDGMENT

The authors thank M. Gao and M. Jansen for their contribution to a part of the experimental work and J. Van Lent, H. Bloksma (Virology Department, Wageningen University), and H. Baptist (Food Physics Group, Wageningen University) for their assistance with the TEM analysis.

LITERATURE CITED

(1) Kavanagh, G. M.; Clark, A. H.; Ross-Murphy, S. B. Heat-induced gelation of globular proteins: part 3. Molecular studies on low pH beta-lactoglobulin gels. *Int. J. Biol. Macromol.* **2000**, *28*, 41–50.

(2) Arnaudov, L. N.; de Vries, R.; Ippel, H.; Van Mierlo, C. P. M. Multiple steps during the formation of beta-lactoglobulin fibrils. *Biomacromolecules* **2003**, *4*, 1614–1622.

(3) Durand, D.; Gimel, J. C.; Nicolai, T. Aggregation, gelation and phase separation of heat denatured globular proteins. *Phys. A* **2002**, *304*, 253–265.

(4) Veerman, C.; Ruis, H.; Sagis, L. M. C.; Van der Linden, E. Effect of electrostatic interactions on the percolation concentration of fibrillar beta-lactoglobulin gels. *Biomacromolecules* **2002**, *3*, 869–873.

(5) Gosal, W. S.; Clark, A. H.; Pudney, P. D. A.; Ross-Murphy, S. B. Novel amyloid fibrillar networks derived from a globular protein: beta-lactoglobulin. *Langmuir* **2002**, *18*, 7174–7181.

(6) Veerman, C.; Schiffart, G. d.; Sagis, L. M. C.; Van der Linden, E. Irreversible self-assembly of ovalbumin into fibrils and the resulting network rheology. *Int. J. Biol. Macromol.* **2003**, *33*, 121–127.

(7) Veerman, C.; Sagis, L. M. C.; Heck, J.; Van der Linden, E. Mesostructure of fibrillar bovine serum albumin gels. *Int. J. Biol. Macromol.* **2003**, *31*, 139–146.

(8) Arnaudov, L. N.; De Vries, R. Thermally induced fibrillar aggregation of hen egg white lysozyme. *Biophys. J.* **2005**, *88*, 515–526.
(9) Akkermans, C.; Van der Goot, A. J.; Venema, P.; Van der Linden, E.; Boom, R. M. Formation of fibrillar whey protein aggregates: influence of heat- and shear treatment and resulting rheology. *Food Hydrocolloids*, in press.
(10) Akkermans, C.; Venema, P.; Rogers, S. S.; Van der Goot, A. J.; Boom, R. M.; Van der Linden, E. Shear pulses nucleate fibril aggregation. *Food Biophys.* **2006**, *1*, 144–150.
(11) Bolder, S. G.; Sagis, L. M. C.; Venema, P.; Van der Linden, E. Effect of stirring and seeding on whey protein fibril formation. *J. Agric. Food Chem.* **2007**, *55*, 5661–5669.
(12) Bolder, S. G.; Hendrickx, H.; Sagis, L. M. C.; Van der Linden, E. Fibril assemblies in aqueous whey protein mixtures. *J. Agric. Food Chem.* **2006**, *54*, 4229–4234.
(13) Scallon, B.; Thanh, V. H.; Floener, L. A.; Nielsen, N. C. Identification and characterization of DNA clones encoding group-II glycinin subunits. *Theor. Appl. Genet.* **1985**, *70*, 510–519.
(14) Fischer, R. L.; Goldberg, R. B. Structure and flanking regions of soybean seed protein genes. *Cell* **1982**, *29*, 651–660.
(15) Lakemond, C. M. M.; de Jongh, H. H. J.; Hessing, M.; Gruppen, H.; Voragen, A. G. J. Heat denaturation of soy glycinin: influence of pH and ionic strength on molecular structure. *J. Agric. Food Chem.* **2000**, *48*, 1991–1995.
(16) Utsumi, S.; Matsumura, Y.; Mori, T. Structure-function relationships of soy proteins. In *Food Proteins and Their Applications*; Damodaran, S., Praf, A., Eds.; Marcel Dekker: New York, 1997; p 257.
(17) Puppo, M. C.; Lupano, C. E.; Anon, M. C. Gelation of soybean protein isolates in acidic conditions - effect of pH and protein concentration. *J. Agric. Food Chem.* **1995**, *43*, 2356–2361.
(18) Hermansson, A. M. Structure of soya glycinin and conglycinin gels. *J. Food Sci. Agric.* **1985**, *36*, 822–832.
(19) Kuipers, B. J.; Koningsveld, G. A. v.; Alting, A. C.; Driehuis, F.; Gruppen, H.; Voragen, A. G. J. Enzymatic hydrolysis as a means of expanding the cold gelation conditions of soy proteins. *J. Agric. Food Chem.* **2005**, *53*, 1031–1038.
(20) Kuipers, B. J. H.; Van Koningsveld, G. A.; Alting, A. C.; Driehuis, F.; Voragen, A. G. J.; Gruppen, H. Opposite contributions of glycinin- and beta-conglycinin-derived peptides to the aggregation behavior of soy protein isolates. *Food Biophys.* **2006**, *1*, 178–188.
(21) Klein, C.; Venema, P.; Sagis, L. M. C.; Van Dusschoten, D.; Wilhelm, M.; Spies, H. W.; Van der Linden, E.; Rogers, S. S.; Donald, A. M. Rheo-optical measurements by fast Fourier transform and oversampling. *Appl. Rheol.* **2007**, *17*, 45210.
(22) Rogers, S. S.; Venema, P.; Sagis, L. M. C.; Van der Linden, E.; Donald, A. M. Measuring the length distribution of amyloid fibrils: a flow birefringence technique. *Macromolecules* **2005**, *38*, 2948–2958.
(23) Aymard, P.; Nicolai, T.; Durrand, D. Static and dynamic scattering of beta-lactoglobulin aggregates formed after heat-induced denaturation at pH 2. *Macromolecules* **1999**, *32*, 2542–2552.
(24) Bolder, S. G.; Sagis, L. M. C.; Venema, P.; Van der Linden, E. Thioflavin T and birefringence assays to determine the conversion of proteins into fibrils. *Langmuir* **2007**, *23*, 4144–4147.
(25) Gittes, F.; Mickey, B.; Nettleton, J.; Howard, J. Flexural rigidity of microtubules and actin filaments measured from thermal fluctuations in shape. *J. Cell Biol.* **1993**, *120*, 923–934.
(26) Doi, M.; Edwards, S. F. Dynamics of rod-like macromolecules in concentrated solution. Part 2. *J. Chem. Soc., Faraday Trans. 2* **1978**, *74*, 918–932.
(27) Krebs, M. R. H.; Bromley, E. H. C.; Donald, A. M. The binding of thioflavin-T to amyloid fibrils: localisation and implications. *J. Struct. Biol.* **2005**, *149*, 30–37.
(28) Sagis, L. M. C.; Veerman, C.; Van der Linden, E. Mesoscopic properties of semiflexible amyloid fibrils. *Langmuir* **2004**, *20*, 924–927.

Received for review June 26, 2007. Revised manuscript received September 6, 2007. Accepted September 10, 2007. This research was financially supported by the Dutch graduate school, VLAG, and the Dutch research programme, Miconed.

JF0718897